Electronic Supplementary Material (ESI) for Journal of Materials Chemistry B.

Supporting Information for

Dual photoisomerization mechanism of azobenzene embedded in a lipid membrane

Silvio Osella[1,2]*, Giovanni Granucci[3], Maurizio Persico[3], Stefan Knippenberg[4,5]*

[1] Chemical and Biological Systems Simulation Lab, Centre of New Technologies, University of Warsaw, Banacha 2C, 02-097 Warsaw, Poland

[2] Materials and Process Simulation Center (MSC), California Institute of Technology, MC 139-74, Pasadena CA, 91125, USA.

[3] Dipartimento di Chimica e Chimica Industriale, Universitá di Pisa, v. Moruzzi 13, I-56124 Pisa, Italy

[4] Hasselt University, Theory Lab, Agoralaan Building D, 3590 Diepenbeek, Belgium

[5] Université Libre de Bruxelles, Spectroscopy, Quantum Chemistry and Atmospheric Remote Sensing (SQUARES), 50 Avenue F. Roosevelt, C.P. 160/09, B-1050 Brussels, Belgium

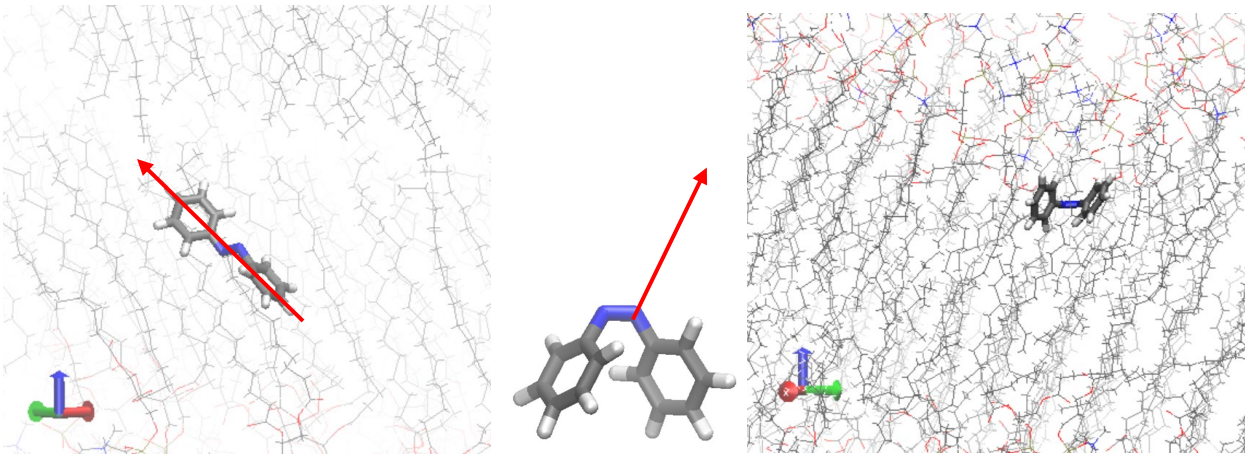

Figure S1. Orientation of the AZO-t (left) and AZO-c (right) at the end of the ground state MD simulation. The red arrow indicate the orientation of the transition dipole moment for both isomers.

1. Charges used in the FF for the two azobenzene isomers

Atom type, atom name and atomic charge used in the FF for the trans and cis isomers.[a]

Trans isomer			Cis isomer		
CAT	CA1	-0.22857	CA	CA1	-0.35516
CAT	CA2	-0.0184	CA	CA2	0.662999
CAT	CA3	-0.3141	CA	CA3	-0.48928
CAT	CA4	0.4659	CA	CA4	-0.00213
CAT	CA5	-0.1469	CA	CA5	-0.1926
CAT	CA6	-0.1095	CA	CA6	-0.0912
HA	H1	0.1488	NAC	N1	-0.3164
HA	H2	0.1153	NAC	N2	-0.3154
HA	H3	0.137101	CA	CA7	0.6613
HA	H4	0.077404	CA	CA8	-0.4851
HA	H5	0.135449	CA	CA9	-0.0045
NAT	N1	-0.26161	CA	CA10	-0.1910
NAT	N2	-0.26411	CA	CA11	-0.09139
CAT	CA7	0.468327	CA	CA12	-0.35732
CAT	CA8	-0.31446	HA	H1	0.194273
CAT	CA9	-0.0186	HA	H2	0.209098
CAT	CA10	-0.2297	HA	H3	0.116837
CAT	CA11	-0.1079	HA	H4	0.135166
CAT	CA12	-0.1487	HA	H5	0.128147
HA	H6	0.1491	HA	H6	0.2079
HA	H7	0.1156	HA	H7	0.1171
HA	H8	0.1372	HA	H8	0.1348
HA	H9	0.07741	HA	H9	0.1282

HA	H10	0.135179	HA	H10	0.1956

[a] The atom numbering and molecular schemes of the (a) trans and (b) cis isomerisations of AZO is given in the depictions here below. CNNC and CNN denote the CA4-N1-N2-CA7 dihedral angle and CA3-CA4-N1 angle, respectively. (c) the DPPC lipid structure is also depicted, (d) the possible photoisomerization mechanisms are shown.

(a)

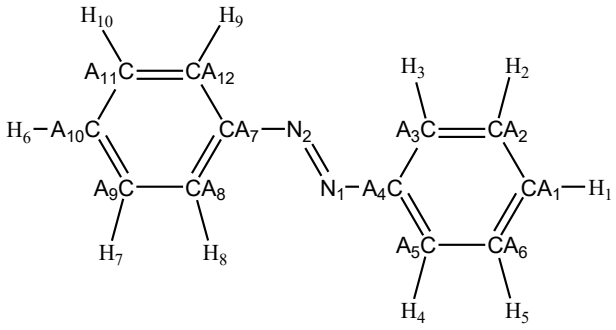

(b)

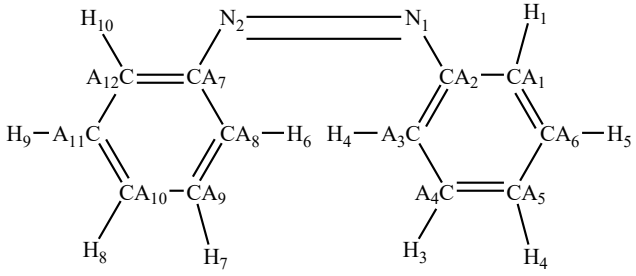

(c) DPPC structure

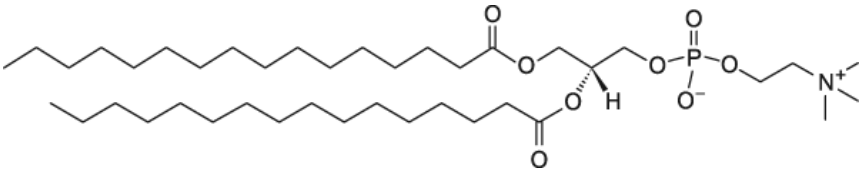

(d)

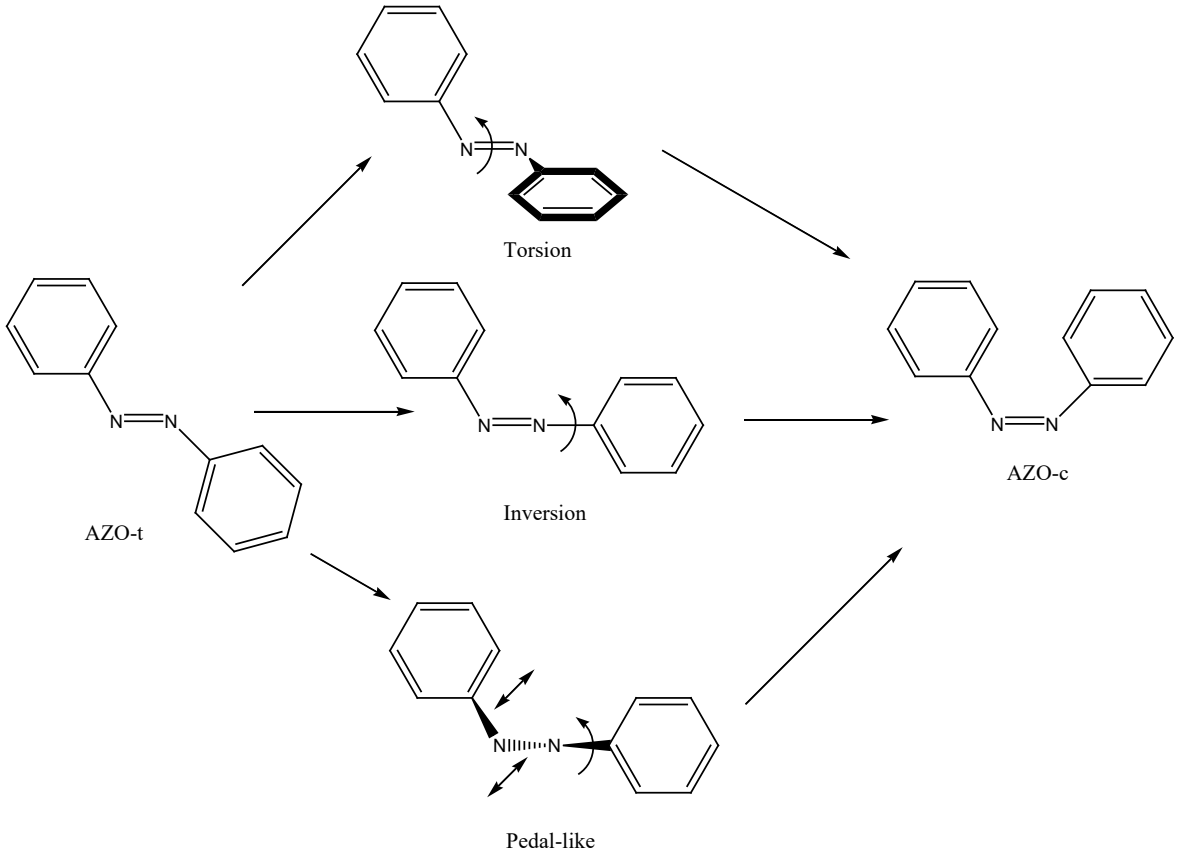

1. Additional methodological details

The QM/MM setting is the following; the azobenzene molecule is considered at the QM level, while a small portion of the environment (DPPC membrane and water molecules) is considered at the MM level of theory in the electrostatic embedding scheme, as described in the main paper. The calculations have been performed by linking MOPAC with the MM package TINKER. The QM/MM interactions are in the form of a Lennard-Jones potential between the MM and the QM atoms, plus electrostatic interactions that are added to the semiempirical Hamiltonian. The electrostatic potential to which the QM nuclei and electrons are subjected is generated by the MM atomic charges.

The surface hopping (SH) was computed considering the AM1 semiempirical method and an open active space of 14 electrons in 13 orbitals (14,13), which allows for fractional occupancy of the molecular orbitals (FOMO) and can be considered as a cheap substitute of CASSCF. The FOMO-CI approach set up by the Persico group is in line with the traditional semiempirical methods based on the neglect of differential overlap (NDO). The main modification introduced in this approach is that the MOs ϕ_i are computed by floating occupation SCF, a pseudo-closed shell SCF where the density matrix is defined in terms of fractional occupation numbers n_i:

$$\rho(r) = \sum_i n_i \, \varphi_i^2$$

which depend on the orbital energies ε_i as

$$n_i = 2 \int_{-\infty}^{\varepsilon_f} g(\varepsilon - \varepsilon_i) d\varepsilon$$

where $g(x)$ is a bell-shaped function (usually a gaussian) normalized to 1, and the Fermi energy ε_f is determined by the requirement that the n_i sum up to the number of electrons.

The SCF calculation is followed by a CI, with a number of configurations and a MO active space as small as possible but such as to ensure a correct treatment of the static correlation. The main advantage of FOMO-CI, apart from the computational speed, is that the results do not depend on the subspace of states that are optimized, and therefore is not prone to the root switching problem. Yet, a downside of this approach is the eventual need to reparametrize the semiempirical Hamiltonian because the commonly used sets (such as MNDO, AM1 and PMn) have been optimized for closed shell HF wavefunctions which only describe ground state properties. However, standard parameter sets provide good starting points and in most cases do not need to be fully reoptimized. The main features of the FOMO-CI direct dynamics, as it is implemented in a development version of the MOPAC 2002 package,[1] can be found in Ref 2.

Through the whole study, we considered the overlap based decoherence correction (ODC), introduced by the Persico Group.[3] Briefly, in mixed quantum–classical methods a major source of error is to assume that the nuclear motion in all the electronic states are represented by the same classical trajectory. In particular, with SH a swarm of trajectories is run starting with different initial conditions and each trajectory is determined by one PES which may change in time due to hops (nonadiabatic events). However, all states do interact through nonadiabatic couplings computed at the current nuclear phase space point. To take into account the vanishing interaction of diverging pathways, the ODC procedure considers a set of ancillary trajectories *(i,j)* for the nuclear motion on every other excited state $l \neq k$. The ancillary trajectories start at different phase space points and, though driven by very simplified potential energy functions, do account realistically for the divergence of pathways on different PESs. Whenever the overlap module $|\langle G(i,j)|G(i,0)\rangle|$ drops below a threshold (S_{min}), the ancillary trajectory *(i,j)* on state *l* is cancelled and the associated probability is attributed to the current state *k*. In this way, the interference between the current state and any other state with diverging trajectories is gradually phased out, which is a way to conjugate the quantum decoherence with the SH model.

2. Area per lipid analysis of equilibrated DPPC alone and with azo at 323 K.

DPPC 0.596 nm^2

AZOt-DPPC 0.53 nm^2

AZOc-DPPC 0.545 nm^2

Exp (323K) 0.631 ± 0.08 nm^2 [4]

With pure DPPC, we can reproduce the exp value within a 5.5% error. The insertion of AZO has quite a strong impact on the as it wobbles and locally disrupt the membrane leading to an error exceeding 13% for cis and 16% for trans.

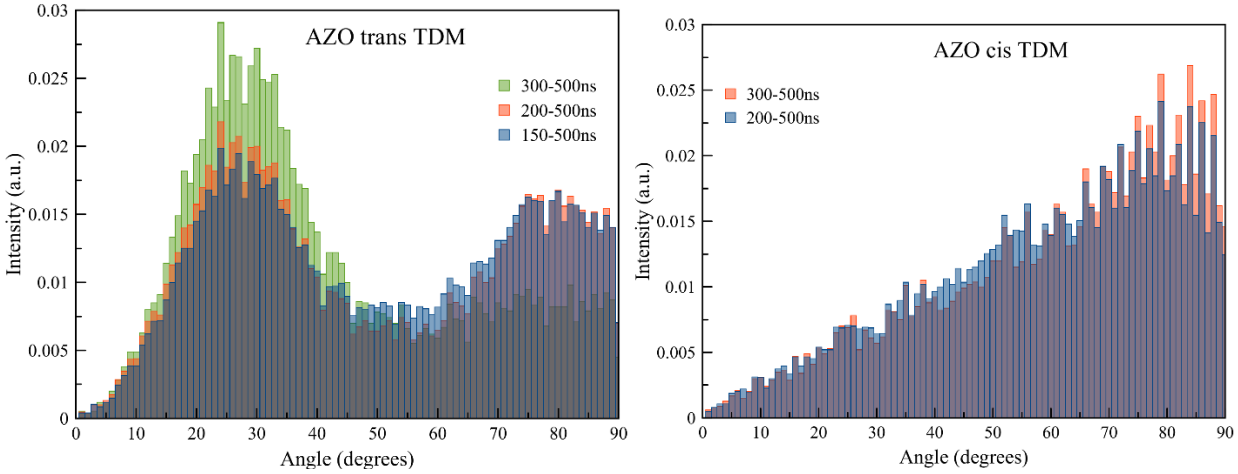

Figure S2. Angle between the tdm and the membrane normal for different time windows. Tdm is considered as the vector between the two C atoms in para to the N=N bond for AZO trans, and as the vector along the C-N bond which makes and angle of 63 degrees with the N=N bond for AZO cis.

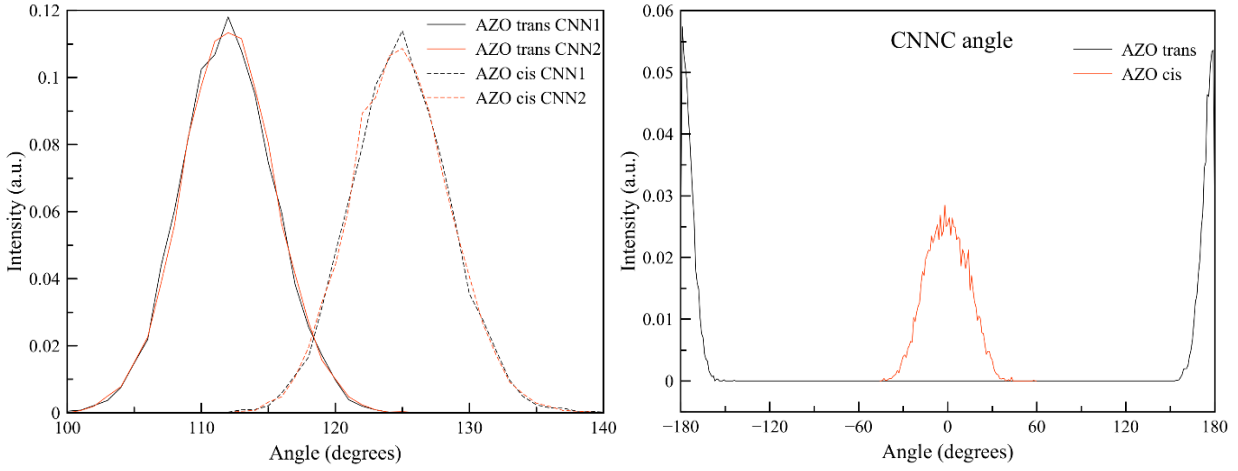

Figure S3. Density plots for (a) the CNN1 and CNN2 angles of trans and cis; and (b) the CNNC dihedral angle.

Table S1. Decay times from exponential fit of population decay time for S_0 (τ_0) and for the S_1 state (τ_1) for the inactive trajectories. Times are reported in ps.

environment	**isomerization**	τ_0	τ_1
vacuum	Trans-cis	0.34	0.34
	Cis-trans	0.06	0.06
DPPC 323K	Trans-cis	1.97	1.97
	Cis-trans	0.07	0.06

Analysis of Photochemical pathway and isomerization mechanism

After the initial excitation of the AZO-t from the ground state to the S_1 state (with average energy at 2.2 eV) and in less than 0.5 ps, the population starts to be transferred to the ground state with no distinction between active and inactive trajectories. A majority of trajectories are then found to stay on the S_1 surface for an extended time interval, presumably due to existence of a local minimum and shallow barrier preceding the S_1/S_0 CoIn at CNNC=100 degrees and to the hindering effect of the environment. All trajectories show a fast non-radiative decay, with some having an early decay character (i.e. they jump to S_0 before reaching the CoIn). While the active trajectories (finishing in the cis ground state surface) show a twisted geometry, with an average CNNC angle of 107 degrees, the inactive ones hop to S_0 further from the CoIn in the torsional coordinate, with an average CNNC angle of 120 degrees. This can be also quantified considering the difference in S_1-S_0 energy. In fact, most reactive trajectories hop with an S_1-S_0 energy difference of less than 0.2 eV. Such small energy differences indicate proximity to the conical intersection, while for the inactive trajectories (the ones returning to the trans ground state), this energy difference is larger (0.33 eV in the average), confirming that these hops occur further from the CoIn and from the transition state that separates AZO-t and AZO-c in the S_0 PES. On average, an overall decay time of 2.23 ps for the inactive trajectories, and of 2.84 ps for the active ones was observed. The long decay time can be directly related to the presence of the DPPC membrane surrounding the AZO-t probe.

In contrast, by starting from the AZO-c ground state isomer and exciting in the S_1 state (with averaged excitation energy of 2.6 eV), in less than 0.5 ps the trajectories reach the conical intersection.

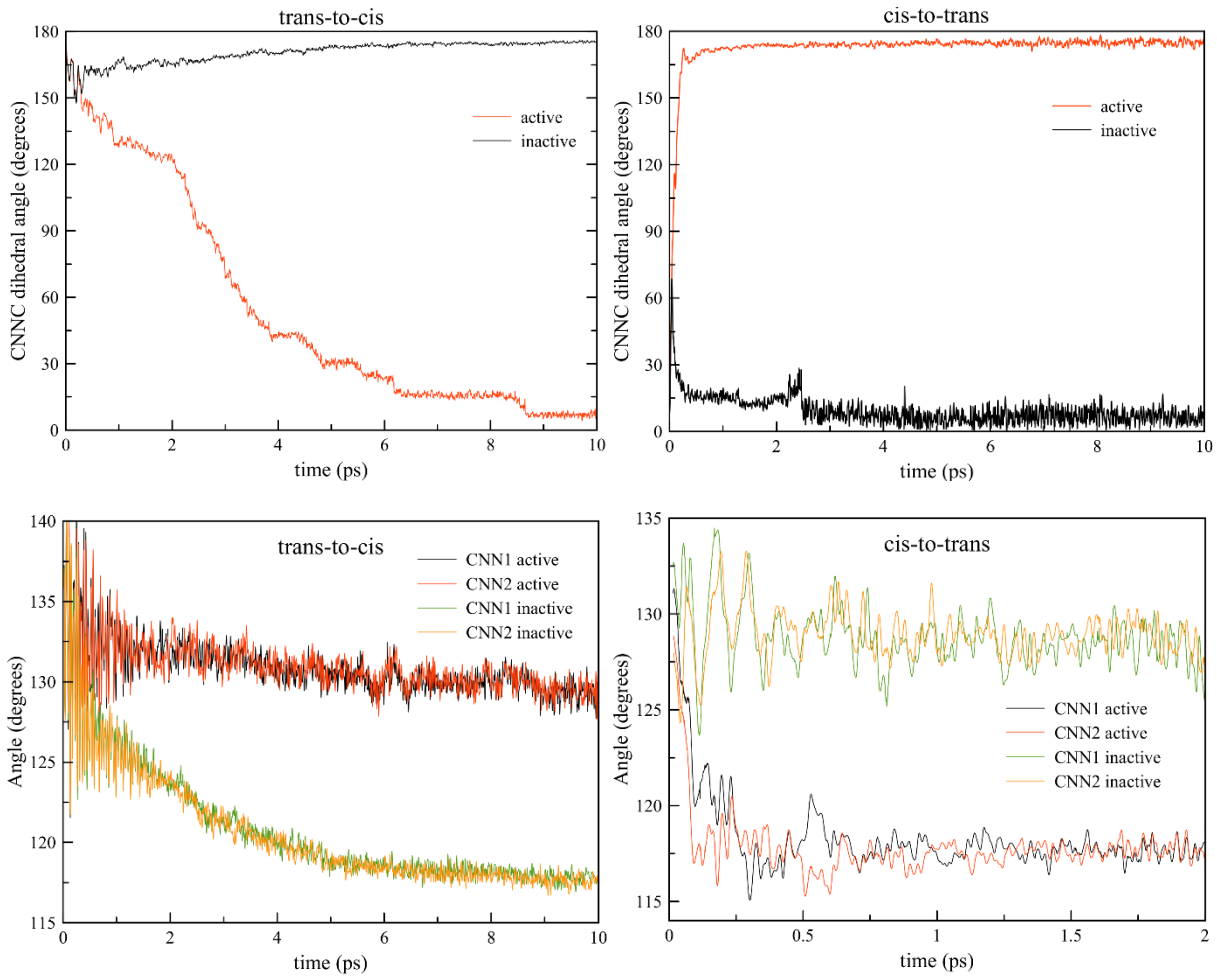

Figure S4. CNNC dihedral (top) and CNN angles (bottom) analysis for the trans to cis (left) and cis to trans decay (right).

Fluorescence anisotropy

An important factor to take into account is the presence of the DPPC environment. The interaction between the probe and the DPPC molecules can be weakened due to the partial conversion of the absorbed photon energy into vibrational excitations, which are then transferred to the environment. Thus, for AZO-t we can consider the rotation mostly hindered, since the probe has not only to lose its planarity and to weaken the probe-environment interaction, but also actively displace the surrounding DPPC molecules to enable the photoisomerization process, thus slowing down also the fluorescence emission and the anisotropy decay.[5] The differences in interplay with the environment become clear when the partial charges of the two N-atoms in the probe are considered. For AZO-t, they amount to -0.25 *e* and -0.28 *e* and are therefore rather limited in terms of electrostatic exchange; the ones for AZO-c are considerably different with values of -0.40 *e* and -0.56 *e*. On the other hand, the AZO-c isomer already presents itself in a more favorable situation, at the edge with the lipid bilayer's head group region, where the density is known to change and where the steric hindrance of the surrounding DPPC molecules is much less pronounced than for the AZO-t. Moreover, the photoisomerization process is now energetically favorable since it will, at the same time, decrease the distortion in the environment and reestablish probe-environment interactions which stabilize the system. This, in turn, is responsible for the fast photoisomerization process, and the strong anisotropy decay.

References

1. J. J.P Stewart MOPAC 2002. Fujitsu Limited, Tokyo (**2002**).
2. M. Persico, G. Granucci, *Theor Chem Acc* 133, 1526 (**2014**).
3. G. Granucci, M. Persico, A. Zoccante *J. Chem. Phys.* 133, 134111/1-9 (**2010**).
4. J. F. Nagle *Biophys J*. 64,1476-81 (**1993**).
5. A. Margineanu, J. Hotta, M. Van der Auweraer, M. Ameloot, A. Stefan, D. Beljonne, Y. Engelborghs, A. Herrmann, K. Müllen, F. C. De Schryver and J. Hofkens, *Biophys. J.* 93, 2877–2891 (**2007**).